Effect of Temperature and the F27W Mutation on the Ca^{2+} Activated Structural Transition of Trout Cardiac Troponin C†

Todd E. Gillis,[‡,§] Tharin M. A. Blumenschein,[||] Brian D. Sykes,[||] and Glen F. Tibbits*[,§,⊥]

Department of Biological Sciences and Cardiac Membrane Research Lab, Simon Fraser University, Burnaby, British Columbia, Canada, Canadian Institutes of Health Research Group in Protein Structure and Function, Department of Biochemistry, University of Alberta, Edmonton, Alberta, Canada, and Cardiovascular Sciences, British Columbia Research Institute for Children's and Women's Health, Vancouver, British Columbia, Canada

Received January 13, 2003

ABSTRACT: The Ca^{2+} sensitivity of cardiac contractile element is reduced at lower temperatures, in contrast to that in fast skeletal muscle. Cardiac troponin C (cTnC) replacement in mammalian skinned fibers showed that TnC plays a critical role in this phenomenon (Harrison and Bers, (1990), *Am. J. Physiol. 258*, C282−8). Understanding the differences in affinity and structure between cTnCs from cold-adapted ectothermic species and mammals may bring new insights into how the different isoforms provide different resistances to cold. We followed the Ca^{2+} titration to the regulatory domain of rainbow trout cTnC by NMR (wild type at 7 and 30 °C and F27W mutant at 30 °C) and fluorescence (F27W mutant, at 7 and 30 °C) spectroscopies. Using NMR spectroscopy, we detected Ca^{2+} binding to site I of trout cTnC at high concentrations. This places trout cTnC between mammalian cTnC, in which site I is completely inactive, and skeletal TnC, in which site I binds Ca^{2+} during muscle activation, and which is not as much affected by lower temperatures. This binding was seen both at 7 and at 30 °C. Despite the low Ca^{2+} affinity, trout TnC site I may increase the likelihood of an opening of the regulatory domain, thus increasing the affinity for TnI. This way, it may be responsible for trout cTnC's capacity to function at lower temperatures.

Functional comparison of mammalian cardiac myofibrils with those isolated from trout reveal that trout cardiac myofibrils were more sensitive to Ca^{2+} as reflected in their ability to generate half-maximal tension at lower [Ca^{2+}] (*1*). To identify the mechanisms responsible for the high sensitivity of trout cardiac myofibrils, we have cloned and sequenced cardiac troponin C (cTnC)[1] from the trout heart (ScTnC) (*2*). The amino acid sequence of this protein is 93% identical to mammalian (human/bovine/porcine isoform) cTnC (McTnC) (*2*). Using F27W mutants in fluorescence studies, we have demonstrated that site II of ScTnC has twice the Ca^{2+} affinity of McTnC (*3*). We believe, therefore, that the higher Ca^{2+} sensitivity of the trout cardiac myofilaments is a consequence of the high Ca^{2+} affinity of ScTnC as it is the binding of Ca^{2+} to cTnC that initiates the contractile reaction and regulates myocyte contractility.

When activated by Ca^{2+}, cTnC undergoes a conformational change that is transferred to the other components of the contractile element, resulting in the formation of force-generating cross-bridges between actin thin filaments and S1 myosin heads. cTnC and fast skeletal TnC (sTnC) are small (18 kDa) dumbbell shaped proteins composed of two globular shaped, Ca^{2+} binding domains separated by an α-helical linker. Each domain contains 2 EF-hand Ca^{2+} binding sites. Sites I and II are low affinity sites and are found in the N-terminal regulatory domain, while sites III and IV are high affinity sites and are located in the C-terminal structural domain. Each EF-hand site is composed of a helix−loop−helix structural motif, in which six residues in the 12-residue loop (at positions 1, 3, 5, 7, 9, and 12, also known as *x*, *y*, *z*, −*y*, −*x*, and −*z*) coordinate to form a pentagonal bipyramid around the Ca^{2+} ion. Residue 12 provides bidentate coordination through both side-chain carboxylate oxygens (*4*). In mammalian cTnC, site I is nonfunctional because of the replacement of charged residues in positions 1 and 3 with hydrophobic residues. While sTnC binds two Ca^{2+} ions in its regulatory domain, it is the binding of a single Ca^{2+} ion to cTnC, through site II, that initiates the change in protein conformation that starts cardiac muscle contraction (*5*). Sites III and IV are considered to have a structural function, helping to anchor TnC into the troponin complex and are always saturated with either Ca^{2+} or Mg^{2+} under physiological conditions.

† Supported by operating grants from the Heart and Stroke Foundation of BC and Yukon (G.F.T.), NSERC of Canada (G.F.T.), and the Canadian Institutes of Health Research (B.D.S.). T.E.G. is the recipient of a Doctoral Fellowship from the Heart and Stroke Foundation of Canada, and T.M.A.B. is the recipient of an Alberta Heritage Foundation for Medical Research Postdoctoral Fellowship.

* To whom correspondence should be addressed. Phone: (604) 291-3658. Fax: (604) 291-3040. E-mail: tibbits@sfu.ca.

‡ Department of Biological Sciences, Simon Fraser University.

§ Cardiac Membrane Research Lab, Simon Fraser University.

|| University of Alberta.

⊥ British Columbia Research Institute for Children's and Women's Health.

[1] Abbreviations: NMR, nuclear magnetic resonance; TnC, troponin C; TnI, troponin I; cTnC, cardiac troponin C; sTnC, fast skeletal troponin C; cNTnC, N-domain of cardiac troponin C; McTnC, mammalian cardiac troponin C; ScTnC, salmonid (trout) cardiac troponin C; [^{15}N] ScNTnC, ^{15}N-labeled N-domain of salmonid (trout) cardiac troponin C; sNTnC, N-domain of fast skeletal troponin C; MALDI-TOF MS, matrix assisted laser desorption/ionization-time-of-flight mass spectrometry.

10.1021/bi0340494 CCC: $25.00
Published on Web 05/08/2003

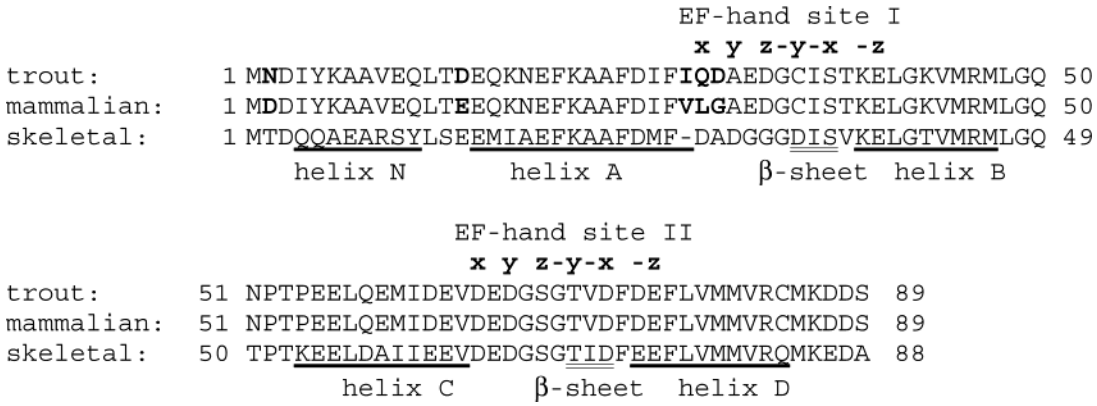

FIGURE 1: Alignment of trout cardiac, mammalian cardiac, and rabbit fast skeletal TnC N-domain sequences. The differences in amino acid sequences between trout and mammalian (human/bovine/porcine isoform) cTnC are shown in bold print. The Ca^{2+}-coordinating positions in each EF-hand site are shown above the sequences.

Comparison of the amino acid sequence of ScTnC and McTnC reveals that site II is completely conserved; however, in the N-terminal domain there are a total of five sequence differences (*2*). These are the replacement of aspartate, glutamate, valine, leucine, and glycine in McTnC by asparagine, aspartate, isoleucine, glutamine, and aspartate in ScTnC, at residues 2, 14, 28, 29, and 30, respectively (Figure 1). By removing the C-terminus of ScTnC and McTnC through creating 1−89 ScTnC and McTnC F27W mutants (F27W ScNTnC and F27W McNTnC) and measuring the ability of these mutants to bind Ca^{2+} at 21 °C, we have demonstrated that the difference in Ca^{2+} affinity is maintained (*6*). This demonstrates, therefore, that the differences in the N-terminus of ScTnC are responsible for its high Ca^{2+} affinity.

In cardiac, but not fast skeletal muscle, a reduction in temperature diminishes the sensitivity of the contractile element for Ca^{2+}. Harrison and Bers (*7*) have demonstrated that the desensitizing effect of temperature on cardiac function is due, at least in part, to the effect of temperature on cTnC. Through the replacement of native cTnC in skinned ventricular trabeculae with recombinant sTnC it was demonstrated that the desensitizing effect of low temperature on tension generation was relieved (*7*). Additionally, by titrating recombinant ScTnC and McTnC we have demonstrated that the Ca^{2+} affinity of both isoforms is decreased at lower temperatures (*3*). The mechanism responsible for this effect of temperature on Ca^{2+} affinity is not known. Previous work by Tsuda et al. (*8*) has demonstrated that the structure of the regulatory domain of chicken sTnC (sNTnC) in the apo state assumes a more closed conformation at low temperatures; however, the effect of this change in protein conformation on Ca^{2+} affinity has not been determined.

In this study, we used 2-D NMR spectroscopy to monitor the protein during Ca^{2+} titration of [^{15}N] ScNTnC at 30 and 7 °C. The regions in the protein that are affected by Ca^{2+} binding were mapped. Li et al. (*9*) have used the same technique to study McNTnC and have demonstrated the effectiveness of this method in characterizing global changes in the molecule as it binds Ca^{2+}. To determine if the Ca^{2+} affinity of the regulatory domains of ScTnC and McTnC are affected similarly as the intact protein by a temperature change, the Ca^{2+} affinity of F27W ScNTnC and F27W McNTnC were measured at 30 and 7 °C, using fluorescence techniques. The effect of the F27W mutation on the functional characteristics of ScNTnC was also characterized by monitoring [^{15}N] F27W ScNTnC during Ca^{2+} titration using 2-D{^{1}H, ^{15}N}-HSQC NMR. Through the NMR titrations, we found that site I is capable of binding Ca^{2+} in ScTnC, albeit at low affinity.

EXPERIMENTAL PROCEDURES

Construction of ScNTnC Mutants. To construct the ScNTnC and F27W ScNTnC mutants, stop codons were introduced into ScTnC and F27W ScTnC cDNA after the serine codon at residue 89 using the Quick Change Site Directed Mutagenesis Kit (Stratagene, La Jolla, CA). These gene constructs had been previously cloned into the pGex expression plasmid from Pharmacia Biotech (Baie d'Urfé, QC, Canada) as described in Gillis et al. (*3*). The existing, parental cDNA inserts were used as templates for the extension of sense and antisense oligonucleotide primers containing the stop codon TAA. The sequence of the 5′ sense oligonucleotide primer used for both inserts was as follows: GGACGACAGCTAAGGGAAAACAGAGG. Cassettes containing the mutation were then made using the restriction enzymes *Sty*I and *Bsm*I (New England Biolabs, Mississauga, ON). Full-length ScTnC and F27W ScTnC cDNA, in pGex, were similarly digested with *Sty*I and *Bsm*I. Following digestion, each cassette and the respective plasmid were purified by gel electrophoresis and the QIAquick Gel Extraction Kit (Qiagen, Mississauga, ON). Products were then ligated using T4 DNA ligase (Gibco BRL, Gaithersburg, MD). The nucleotide sequences of the two newly mutated inserts were confirmed by sequencing at the University of British Columbia, Nucleic Acid/Protein Service Unit (Vancouver, BC) using AmpliTaq Dye Terminator Cycle Sequencing.

Expression and Purification of ^{15}N labeled ScNTnC. The pGex plasmids containing the ScNTnC and F27W ScNTnC were transformed into the *Escherichia coli* strain BL21 and ^{15}N labeled protein expressed according to Gagné et al. (*10*) and purified as described by Gillis et al. (*3*). [^{15}N] ScNTnC and [^{15}N] F27W ScNTnC were then desalted according to Li et al. (*11*). The identity of ScNTnC and F27W ScNTnC were confirmed by N-terminal amino acid microsequencing and amino acid analysis completed at the University of British Columbia, Nucleic Acid/Protein Service Unit (Vancouver, BC). The purity of the isolated proteins as well as their atomic masses were confirmed by matrix assisted laser desorption/ionization-time-of-flight mass spectrometry (MAL-

DI-TOF MS) completed at the UBC Mass Spectrometry Center. Collectively, these tests established the identity of [^{15}N] ScNTnC and [^{15}N] F27W ScNTnC.

Expression and Purification of F27W ScNTnC and F27W McNTnC. The pGex plasmids containing the F27W ScNTnC and F27W McNTnC inserts were transformed into the *Escherichia coli* strain BL21 for protein expression. The cTnC isoforms were expressed and purified as described previously (*3*). The identities of the cTnC isoforms were confirmed by MALDI-TOF MS completed at the UBC Mass Spectrometry Centre.

Ca^{2+} Titrations of [^{15}N] ScNTnC at 30 and 7 °C and [^{15}N] F27W ScNTnC at 30 °C Monitored by 2-D {^{1}H, ^{15}N}-HSQC Spectra. Three separate titrations were completed. These were [^{15}N] ScNTnC at 30 and 7 °C and [^{15}N] F27W ScNTnC at 30 °C. To prepare for each titration, the respective desalted protein was dissolved into approximately 500 μL of NMR buffer (100 mM KCl, 10 mM imidazole in 90% H_2O/10% D_2O), to which NaN_3 to 0.03%, dithiothreitol to 20 mM, and 2,2-dimethyl-2-silapentane-5-sulfonic acid to 0.2 mM were added. The concentrations, as determined by amino acid analysis, of [^{15}N] ScNTnC used in the titrations at 30 and 7 °C were 1.3 mM, and the concentration of [^{15}N] F27W ScTnC titrated at 30 °C was 1. 8 mM.

Three $CaCl_2$ stock solutions were used for all titrations, 50, 100, and 1068.5 mM. Gilson pipettors (P2, P10, and P20) were used for all the $CaCl_2$ solution additions. For the titration of [^{15}N] ScNTnC at 30 °C, appropriate aliquots of 50 mM $CaCl_2$, 100 mM $CaCl_2$, and 1068.5 mM $CaCl_2$ were added consecutively to the NMR tube for 28 individual titration points, to a maximum [Ca^{2+}] of 180 mM. During the titration, a total of 1.3 μL of 1 M NaOH was added to maintain pH between 6.8 and 6.9. The total volume changed from 502.5 before titration to 619.2 μL after titration. For the titration of [^{15}N] ScNTnC at 7 °C, appropriate aliquots of 50 mM $CaCl_2$, 100 mM $CaCl_2$, and 1068.5 mM $CaCl_2$ were added consecutively to the NMR for 25 individual titration points, reaching a maximum [Ca^{2+}] of 102 mM. The total volume changed from 500.8 before titration to 565.9 μL after titration. For the titration of [^{15}N] F27W ScNTnC at 30 °C, appropriate aliquots of 50 mM $CaCl_2$, 100 mM $CaCl_2$, and 1068.5 mM $CaCl_2$ were added consecutively to the NMR tube for 25 individual titration points, reaching a maximum [Ca^{2+}] of 102 mM. During the titration, a total of 1.5 μL of 1 M NaOH was added to maintain pH between 6.8 and 6.9. The total volume changed from 500.8 before titration to 565.9 μL after titration. 2-D {^{1}H, ^{15}N}-HSQC spectra were acquired at every titration point for all three proteins. The changes in protein and Ca^{2+} concentrations because of dilutions were taken into account for data analysis.

NMR Spectroscopy. All 2-D {^{1}H,^{15}N}-HSQC spectra were acquired on a Varian Unity 600 MHz spectrometer as described by Li et al. (*9*). ^{1}H, ^{15}N sweep widths were 8000 and 1650 Hz, respectively; NMR spectra were obtained at either 30 or 7 °C. The NMR data were processed using the software package NMRPipe (*12*), and the spectra were analyzed with the software package NMRView (*13*).

Solutions Used in Fluorescence Studies. The solutions used to measure fluorescence at 7 °C, pH 7.0 and 30 °C, pH 7.0 were identical to those described in Gillis et al. (*3*) and contained 1.0 mM EGTA, 0.03 mM $CaCl_2$, 112.0 mM KCl, and 50 mM MOPS. A miniature Ca^{2+} electrode, made according to Baudet et al. (*14*), was used to confirm the purity and apparent Ca^{2+} affinity constant (K'_{Ca}) of the EGTA used in the solution under the experimental conditions. This electrode was also used to test the initial pCa of the solution used in the fluorescence measurements and the change in pCa during Ca^{2+} titration. This electrode was calibrated using Ca^{2+} standards (Orion Research Incorporated, Boston, MA) of pCa 2−5 and produced a standard Nerstian slope of ∼29 mV/pCa unit. The output of the electrode was read with an Orion model EA940 Expandanable IonAnalyzer pH meter. Using this standard curve and solutions containing EGTA, this electrode was accurate to a pCa of ∼8.0. The pCa of both solutions, at the conditions under which they were to be used were measured with the electrode during Ca^{2+} titration and expressed in mV. These data along with the corresponding total [Ca^{2+}] values and Ca^{2+} electrode calibration data were used to calculate the concentration of Ca^{2+} bound to EGTA and the ratio of bound Ca^{2+} to free Ca^{2+} according to the method of Bers et al. (*15*). Scatchard plots of these data were used to determine K'_{Ca}. At 7 °C, pH 7.0 the K'_{Ca} of the EGTA was 1.01×10^6 while at 30 °C, pH 7.0 this value was 2.20×10^6.

Fluorescence Studies. The fluorescence studies were carried out as previously described (*3*) using a Photon Technology International Model c-30 spectrofluorometer (London, ON) attached to a NesLab (Portsmouth, NJ) water bath to maintain the cuvette at 7.0 ± 0.1 and 30.0 ± 0.2 °C.

Fluorescence Data Manipulation and Statistical Analysis. The Ca^{2+}-dependent component of the fluorescence measurements from each titration were determined by subtracting the fluorescence at basal [Ca^{2+}] from all measurements and then expressing the resultant values as a percentage of the maximum fluorescence. Each data set was fitted using the Hill equation with the program Origin 6.0. (Microcal Software Inc., Northhampton, MA) as previously described (*3*). The χ^2, which was used as a goodness-of-fit index of the Hill equation to our data, ranged from 0.0017 ± 0.0004 (McNTnC at 30 °C) to 0.0003 ± 0.0001 (ScNTnC at 30 °C). The effects of isoform and temperature on the pCa_{50} values (Ca^{2+} concentration, in pCa at half-maximal fluorescence) determined by the Hill equation curve fitting were analyzed statistically using a one-way repeated measures analysis of variance (ANOVA) followed by Bonferroni post hoc tests using the statistical software package SigmaStat. The values reported for pCa_{50} are expressed as mean ± SE in pCa units. Two means were considered to be significantly different when the p value was less than 0.05.

RESULTS

Ca^{2+} Titrations Followed by NMR Spectroscopy. The 2-D {^{1}H,^{15}N}-HSQC NMR spectra acquired during the Ca^{2+} titrations of [^{15}N] ScNTnC at 7 and 30 °C and [^{15}N] F27W ScNTnC at 30 °C were well-resolved at every titration point. Figure 2 shows the superposition of a region of the 2-D {^{1}H,^{15}N}-HSQC spectra of [^{15}N] ScNTnC at 7 and 30 °C, in the apo and one-Ca^{2+}-bound states, and of [^{15}N] ScNTnC and [^{15}N] F27W ScNTnC at 30 °C in the apo and one-Ca^{2+}-bound states. As the ratio of $[Ca^{2+}]_{total}/[cNTnC]_{total}$ increased during the titration, the cross-peaks shifted in the ^{1}H and/or ^{15}N dimensions, reflecting changes in their local environments and therefore which residues were the most affected

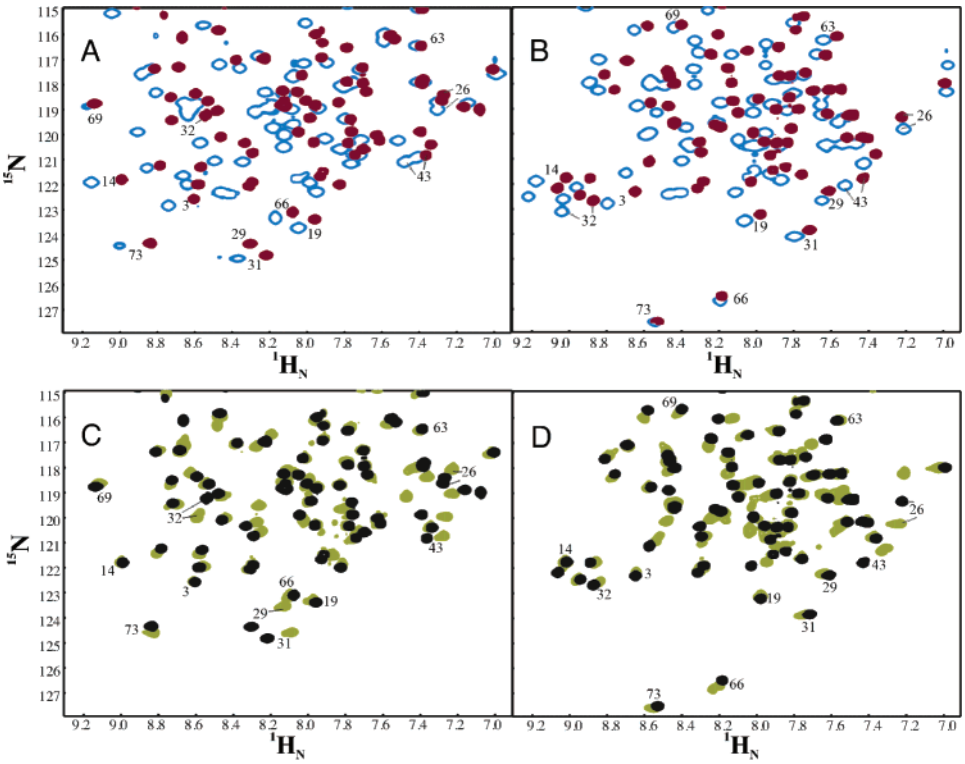

FIGURE 2: Superposition of a region of the 2-D {^{15}N-^{1}H}-HSQC spectra of [^{15}N] ScNTnC at 7 and 30 °C and of [^{15}N] ScNTnC and [^{15}N] F27W ScNTnC at 30 °C. Some assignments are indicated with the residue number. (A) Apo [^{15}N] ScNTnC at 7 °C (in open blue contours) and 30 °C (in red); (B) Ca^{2+}-bound [^{15}N] ScNTnC at 7 and 30 °C; (C) Apo [^{15}N] ScNTnC (in black) and [^{15}N] F27W ScNTnC (in green) at 30 °C; and (D) Ca^{2+}-bound [^{15}N] ScNTnC and [^{15}N] F27W ScNTnC at 30 °C.

by the binding of Ca^{2+}. The chemical shift changes occurred throughout the sequence, indicating that increased Ca^{2+} concentrations cause global changes in the proteins. The total chemical shift change ($\Delta\delta_{total}$) was calculated from the chemical shift changes in both dimensions ($\Delta\delta_H$ and $\Delta\delta_N$) using eq 1 (*16*).

$$\Delta\delta_{total} = \sqrt{(\Delta\delta_{15_N})^2 + (\Delta\delta_{1_H})^2} \qquad (1)$$

When McNTnC is titrated with Ca^{2+} at 30 °C, the peaks stop shifting when the $[Ca^{2+}]_{total}/[cNTnC]_{total}$ reaches 1 (*9*). During the ScNTnC titration, however, the peaks kept shifting when the $[Ca^{2+}]_{total}/[cNTnC]_{total}$ was greater than 1, suggesting the existence of a second binding site.

Gly 34 is located in site I, and its chemical shift changes reflect the binding of Ca^{2+} to both sites. The chemical shift changes of G34 of [^{15}N] ScNTnC at 7 and 30 °C and [^{15}N] F27W ScNTnC at 30 °C were plotted as a function of the $[Ca^{2+}]_{total}/[ScNTnC]_{total}$ ratio and are shown in Figure 3A, and with an expanded abscissa in Figure 3B. These plots have an initial rapid change, corresponding to Ca^{2+} binding to site II. A plot of the chemical shift changes for each residue (Figure 4A−C) shows that the residues that underwent the largest chemical shift change during this period of the titration are those that compose Ca^{2+} binding sites I and II. The plots of the chemical shift change for G34 did not level off once they reached a maximum but began to descend as the $[Ca^{2+}]_{total}/[ScNTnC]_{total}$ ratio increases, demonstrating that the proteins continued to respond to increasing Ca^{2+} concentrations (Figure 3A). This result is different than what has been previously demonstrated by Li et al. (*9*) for McNTnC at 30 °C. These authors demonstrated that all resonances in the spectra had stopped moving when the $[Ca^{2+}]_{total}/[cNTnC]_{total}$ reached unity (*9*). The Ca^{2+} titration curve and data for G70 from this experiment has been superimposed on Figure 3B. The behavior of G70 in McNTnC after saturation of site II was similar to that of all residues throughout the protein in that its position in the 2-D spectra remained constant after $[Ca^{2+}]_{total}/[cNTnC]_{total}$ reached 1 (*9*). To allow comparison between the data for McNTnC and ScNTnC at 30 °C, a spline curve has been fitted to the data for ScNTnC. Although the difference between the two curves seems small, the difference in Figure 3B corresponds to a displacement of 15 Hz for the residues that moved the most, and such a displacement could clearly be seen in the NMR spectra.

The total chemical shift change of each residue in the second phase of the titration demonstrated that chemical shift changes occurred throughout the sequence in all three titrations (Figure 5A−C). The largest changes occurred in the EF-hand site I and some specific residues in EF-hand site II (residues 64 and 70). In all the titrations, $CaCl_2$ was added until the peaks could not be followed anymore because of broadening and loss of signal due to the increase in volume of the NMR sample. That resulted in $[Ca^{2+}]_{total}/[ScNTnC]_{total}$ ratios between 65 and 171. For Figure 5, because of differences in protein concentration, the $[Ca^{2+}]_{total}/[ScNTnC]_{total}$ ratio was about 85 for wild type [^{15}N] ScNTnC at both temperatures and about 65 for [^{15}N] F27W ScNTnC. Therefore, the size of the chemical shift changes is not totally comparable between wild type and [^{15}N] F27W ScNTnC. In none of the three titrations did the Ca^{2+} binding plot of

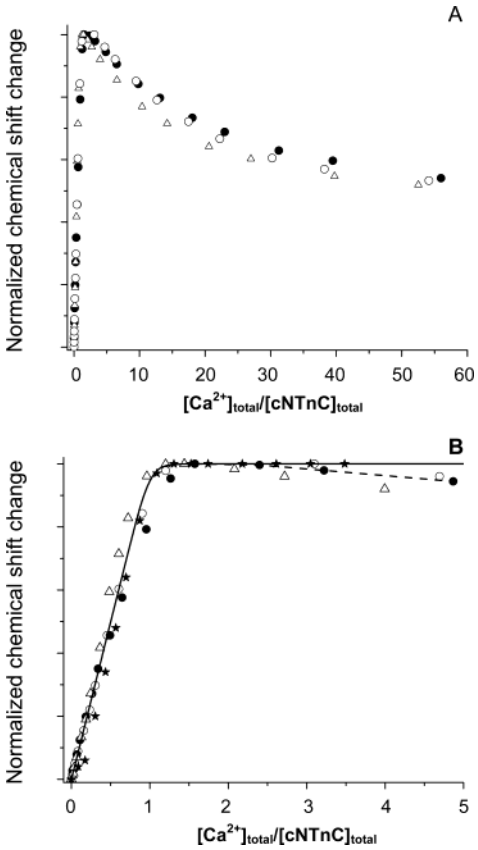

FIGURE 3: Ca^{2+} titration plots of G34 of [^{15}N] ScNTnC at 7 and 30 °C and of [^{15}N] F27W ScNTnC at 30 °C. The data are normalized according to $(\delta_{obs} - \delta_{initial})/(\delta_{1Ca} - \delta_{initial})$. (A) [^{15}N] ScNTnC at 7 °C (open circle), [^{15}N] ScNTnC at 30 °C (closed circle), and [^{15}N] F27W ScNTnC at 30 °C (triangle) with $[Ca^{2+}]_{total}/[cNTnC]_{total}$ from 0 to 60. (B) Expanded view of plot in panel A superimposed on the Ca^{2+} binding curve and data points of G70 McNTnC at 30 °C (star) as determined by Li et al. (*11*). A spline curve (dashed line) has been fitted to the data for ScNTnC at 30 °C, after $[Ca^{2+}]_{total}/[cNTnC]_{total} = 1$, to allow comparison with the data from McNTnC at 30 °C. $[Ca^{2+}]_{total}/[cNTnC]_{total}$ is from 0 to 5.

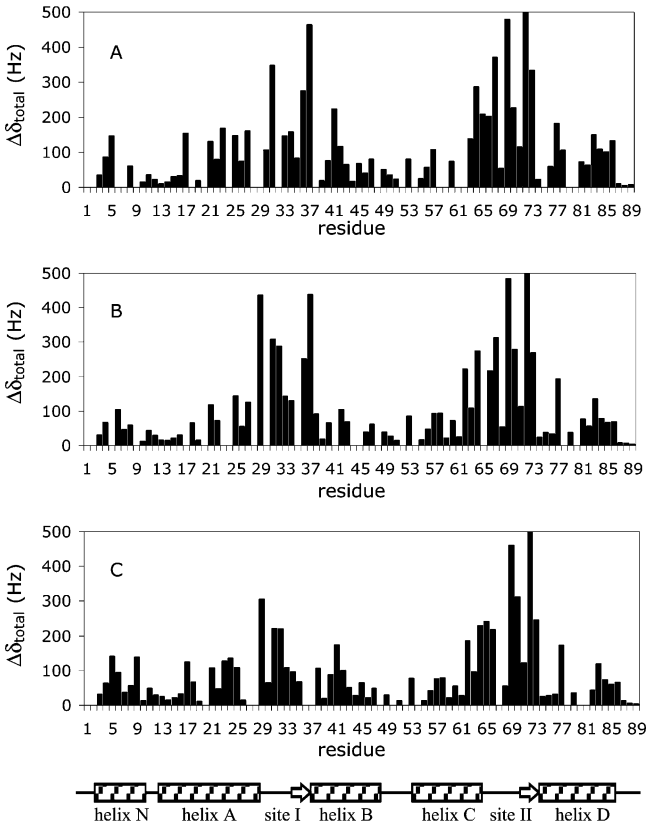

FIGURE 4: Effect of titration on the backbone amide ^{1}H and ^{15}N NMR chemical shift, from apo to one-Ca^{2+} state. The total chemical shift changes ($\Delta\delta_{total}$, in Hz) were calculated according to eq 1. (A) Wild-type [^{15}N] ScNTnC at 7 °C; (B) wild-type [^{15}N] ScNTnC at 30 °C; and (C) F27W [^{15}N] ScNTnC at 30 °C. It was not possible to assign all the peaks during the whole titration, and for that reason the chemical shift changes could not be measured for some residues. The schematic drawing at the bottom shows the structural features along the sequence.

G34 ever become parallel to the *x* axis, reflecting the fact that site I did not become fully saturated under these conditions.

In Figure 6, the net chemical shift of each residue during each phase of all titrations was mapped onto the solution structure of McNTnC (*17*). The binding of the first Ca^{2+} (Figure 6A) causes changes all over the protein, more intense at the two EF-hand sites. On the other hand, the binding of the second Ca^{2+} (Figure 6B) affects mostly site I and helices B and D.

The tight binding of Ca^{2+} to site II, in the high protein concentration used in NMR experiments, precludes precise binding constant measurements by NMR. In Figure 3B, the initial slope of the curve is related to the affinity. The slopes of all curves are within a 10% difference of each other and cannot be differentiated within the protein concentration error. For this reason, no binding constants were determined using the NMR data. However, from the binding curves in Figure 3, the dissociation constants (K_d) can be estimated to be around pCa 5, for site II, and between pCa 2 and 3, for site I.

Temperature Effects on Wild-Type [^{15}N] ScNTnC Chemical Shifts. With decreasing temperatures, most of the {^{1}H, ^{15}N}-HSQC cross-peaks shift slightly downfield, both in the $^{1}H_N$ (maximum of 0.2 ppm) and ^{15}N (less than 0.8 ppm) dimensions (Figure 2A,C). These changes occur both in the presence and in the absence of Ca^{2+} and are different from the changes seen during the Ca^{2+} titration at either temperature.

The temperature coefficient was calculated for wild type [^{15}N] ScNTnC both in the apo and in the one-Ca^{2+} states and plotted in Figure 7. The temperature coefficient is given by $-\Delta\delta_H/\Delta T$, in parts per billion per Kelvin, where $-\Delta\delta_H$ is the difference in the amide proton NMR chemical shift, and ΔT is the difference in temperature, in Kelvin.

In small peptides, plots of the amide ^{1}H NMR chemical shift against the temperature are linear. The slope of such plots is the temperature coefficient and can correlate with the existence of hydrogen bonds (*18*, *19*). This correlation is not as strong in α helices as in other secondary structures (*19*). Since TnC is a highly α-helical protein, it is not surprising that the temperature coefficients do not seem to correlate with the secondary structure elements.

The temperature coefficients do not match the ones for sNTnC (*8*), suggesting that although the overall fold is very similar between the cardiac and the fast skeletal isoforms of TnC (*20*, *21*), there are differences in the details of how the nuclei interact within the protein. Many of the residues could not be assigned in the apo state, making it especially difficult

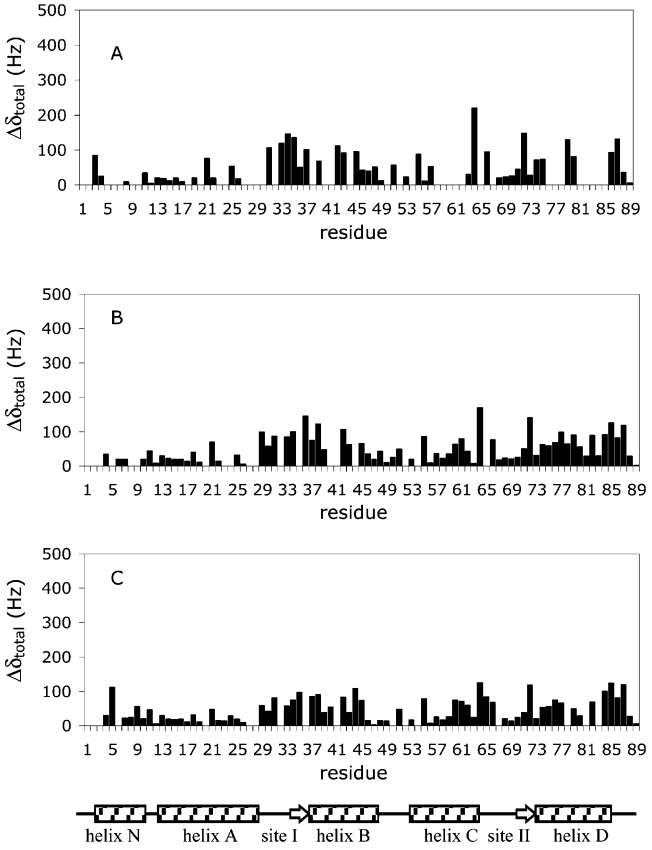

FIGURE 5: Effect of titration on the backbone amide ^1H and ^{15}N NMR chemical shift, from one-Ca^{2+} to two-Ca^{2+} state. The total chemical shift changes ($\Delta\delta_{total}$, in Hz) were calculated according to eq 1. (A) Wild-type [^{15}N] ScNTnC at 7 °C; (B) wild-type [^{15}N] ScNTnC at 30 °C; and (C) F27W [^{15}N] ScNTnC at 30 °C. The $[Ca^{2+}]_{total}/[cNTnC]_{total}$ ratio was about 85 for wild-type [^{15}N] ScNTnC at both temperatures and 65 for F27W [^{15}N] ScNTnC. It was not possible to assign all the peaks during the whole titration, and for that reason the chemical shift changes could not be measured for some residues. The schematic drawing at the bottom shows the structural features along the sequence.

to compare with the skeletal data (available only in the apo state). Out of the seven positive temperature coefficients observed in skeletal NTnC, only one (R83) had the temperature coefficient for the equivalent residue determined in [^{15}N] ScNTnC, and it was negative. The only residue with an observed positive temperature coefficient for apo [^{15}N] ScNTnC was K86, raising the possibility that it is involved in interactions similar to the ones for R83 in skeletal NTnC.

In the one-Ca^{2+} state, three residues had positive temperature coefficients (I26, D67, and V79), which can be caused by local structure changes between the two temperatures. I26 and V79 are both located close to aromatic residues, and changes in the distance between the amide and the aromatic rings have been suggested as a mechanism to cause positive temperature coefficients (*19*).

Effect of the F27W Mutation on [^{15}N] ScNTnC. Superposition of the spectra for [^{15}N] ScNTnC and [^{15}N] F27W ScNTnC at 30 °C in the apo and Ca^{2+}-bound states demonstrates that there are differences in the position of a number of the cross-peaks in the spectra (Figure 2C,D). These differences were measured and are presented in Figure 8. For the apo state, the differences occur mostly in the residues that compose site I (Figure 8A), close to the FW mutation. These differences decrease greatly when site II is saturated, being replaced by differences in the beginning of helix B.

Table 1: pCa_{50} (pCa at Half-Maximal Fluorescence) of Ca^{2+} Binding to F27W ScNTnC and F27W McNTnC at 30.0 °C, pH 7.0 and 7.0 °C, pH 7.0 Determined Using Spectrofluorometry[a]

conditions	F27W ScNTnC	F27W McNTnC
30 °C, pH 7.0	6.46 ± 0.05 (9)	6.14 ± 0.07 (6)
7 °C, pH 7.0	5.59 ± 0.02 (8)	5.42 ± 0.02 (9)

[a] Values are means ± SE; numbers of experiments are in parentheses. All values are significantly different from each other ($p < 0.05$).

In the one-Ca^{2+} state, most peaks were in very similar positions when comparing [^{15}N] ScNTnC and wild type F27W [^{15}N] ScNTnC. In the apo state, however, wild type peaks in site I were more distant from the one-Ca^{2+} position, while F27W peaks were closer. This suggests that [^{15}N] F27W ScNTnC has to undergo smaller conformational changes in site I, when Ca^{2+} binds to site II, than wild type [^{15}N] ScNTnC.

Ca^{2+} Affinity Measurements Using Fluorescence. The Ca^{2+} titration curves of F27W ScNTnC were shifted to the left of those for F27W McTnC at both 30 and 7 °C (Figure 9A,B) indicating that F27W ScNTnC has a higher affinity for Ca^{2+}. Using the pCa_{50} (pCa at half-maximal fluorescence) as a measure of affinity confirms this. At 30 °C, the pCa_{50} of F27W ScNTnC was 0.39 pCa units higher than that of F27W McNTnC, while at 7 °C the difference was 0.17 pCa units (Table 1). A reduction in temperature desensitized both F27W ScNTnC and F27W McNTnC as the concentration of free Ca^{2+} required to half saturate both proteins increased. The pCa_{50} of F27W ScNTnC at 7.0 °C was 0.87 pCa units lower than when measured at 30 °C while the same reduction in temperature lowered the pCa_{50} of F27W McNTnC by 0.72 pCa units.

DISCUSSION

The changes detected in all 2-D {^1H, ^{15}N}- HSQC spectra during the Ca^{2+} titrations were similar to those previously demonstrated for [^{15}N] McNTnC at 30 °C (*9*), using similar NMR techniques. As in [^{15}N] McNTnC, the greatest absolute changes occurred in the residues that compose Ca^{2+} binding sites I and II. Where [^{15}N] ScNTnC and [^{15}N] F27W ScNTnC differ from McNTnC is the fact that global changes continue to occur throughout these proteins after site II is saturated. In McNTnC, all resonances in the spectra were completely saturated when the $[Ca^{2+}]_{total}/[cNTnC]_{total}$ reached unity (*9*). The greatest chemical shift after site II had become saturated in ScNTnC occurred in the residues composing site I and isolated residues in site II, indicating that these residues were most affected by the increasing Ca^{2+} concentration. Li et al. (*9*) demonstrated in McNTnC that once site II became Ca^{2+} saturated, all chemical shift changes of ^{15}N and ^1H_N throughout the spectra stopped. This result is consistent with only site II being able to bind Ca^{2+} in McNTnC. Additionally, titration of a [^{15}N] sNTnC mutant (E41A) in which site I was mostly inactivated but showed residual binding, behaved similarly to [^{15}N] ScNTnC and [^{15}N] F27W ScNTnC in that chemical shift changes continued to occur throughout the sequence after site II became saturated (*9*). The results of the present study therefore suggest that site I is capable of binding Ca^{2+} in both [^{15}N] ScNTnC and [^{15}N] F27W ScNTnC at high Ca^{2+}concentrations.

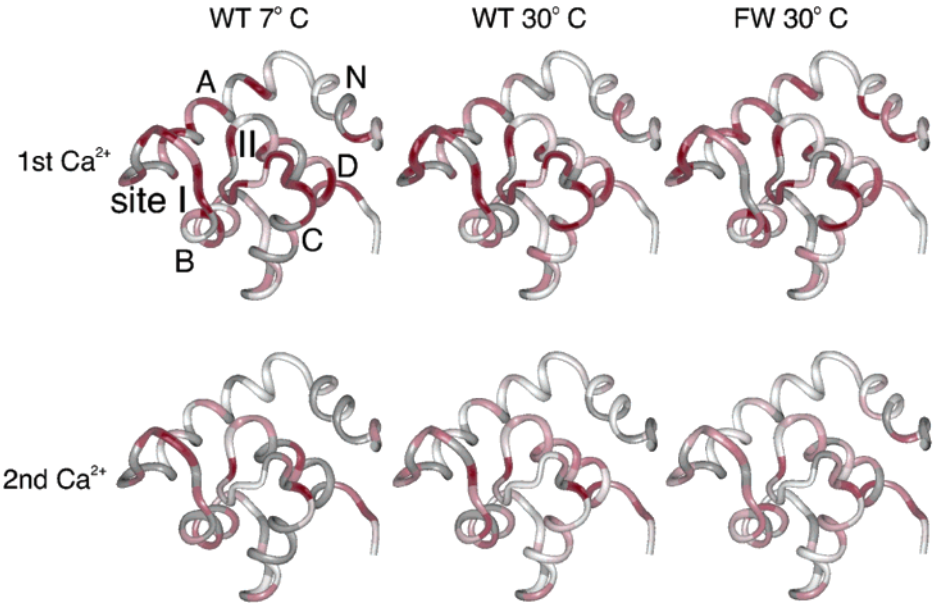

FIGURE 6: Mapping of the residues affected by Ca^{2+} binding to ScNTnC at 7 and 30 °C and F27W ScNTnC at 30 °C. The mapping was done using the structure determined by Spyracopoulos et al. (*17*). The ribbon structure was colored according to how much the amide cross-peak for that residue moved during the Ca^{2+} titration. The residues colored in white moved less than 20 Hz, while the residues purely in red moved more than 150 Hz. The residues in gray could not be measured.

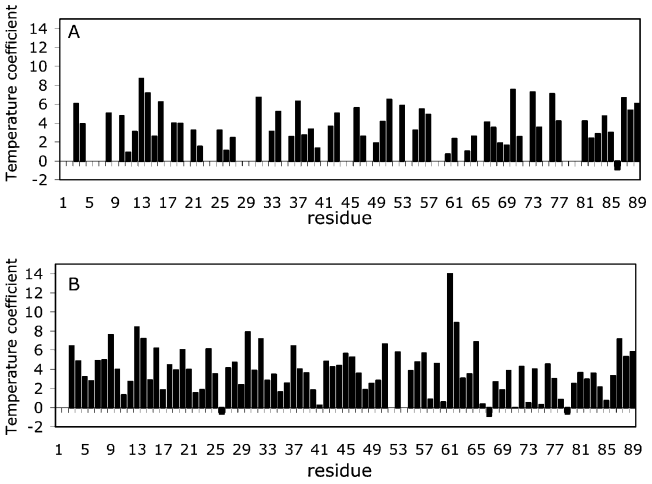

FIGURE 7: Effects of temperature on the backbone amide ^1H NMR chemical shift. Temperature coefficients are defined as $-\Delta\delta_H/\Delta T$. (A) Temperature coefficients (parts per billion per Kelvin) for the backbone amide protons of apo wild-type [^{15}N] ScNTnC. (B) Temperature coefficients (parts per billion per Kelvin) for the backbone amide protons of wild-type [^{15}N] ScNTnC bound to one Ca^{2+} ion. It was not possible to assign all the peaks during the entire titration, and for that reason the temperature coefficients in the apo state could not be measured for some residues.

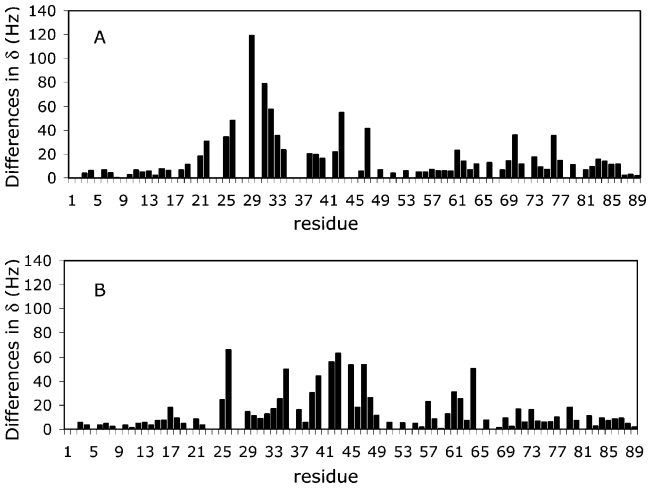

FIGURE 8: Effect of the F27W mutation on the backbone amide ^1H and ^{15}N NMR chemical shifts of [^{15}N] ScNTnC. The bars represent the difference in chemical shift (δ) between the F27W mutant and the wild type [^{15}N] ScNTnC, calculated according to eq 1. (A) In the apo state and (B) bound to 1 Ca^{2+} ion. It was not possible to assign all the peaks during the whole titration, and for that reason the chemical shift changes could not be measured for some residues.

The two positions in site II that suffered the largest chemical shift change during the binding of the second Ca^{2+} ion were Thr 71 and Val 64. Thr 71 is part of the antiparallel β sheet that connects the two EF-hand sites and can be affected by Ca^{2+} binding in site I. Val 64 is the equivalent of Val 65 in sTnC, one of the two hinge residues for the Ca^{2+}-induced opening of the BC helices (*22*). This suggests the possibility of an opening of the BC helices induced by the binding of the second Ca^{2+} ion. The moderate chemical shift changes seen in residues from helix D during the binding of the second Ca^{2+} ion support this hypothesis since an opening of the BC helices would expose helix D. The open and closed states of TnC are characterized by the angle between the BC helices and the rest of the N-terminal domain. The opening of sTnC upon binding of Ca^{2+} is well-documented, but McTnC does not open in the absence of TnI, even in the presence of Ca^{2+}. In ScTnC, the differences in site I may change the equilibrium in favor of the open state, increasing the affinity for TnI.

The sequence differences between rabbit fast skeletal, mammalian cardiac, and trout cardiac TnC can be seen in Figure 1. The first three residues in site I in both mammalian and trout cTnC are very different from sTnC. In McTnC, Ca^{2+}-binding positions *x* and *y* are occupied by hydrophobic residues, therefore losing the ability to bind Ca^{2+}. In ScTnC, the first two positions of the site are occupied by polar residues. Position *x* is occupied by a Gln. Although 98% of the EF-hand sites have an Asp in position *x* (*23*), Gln is

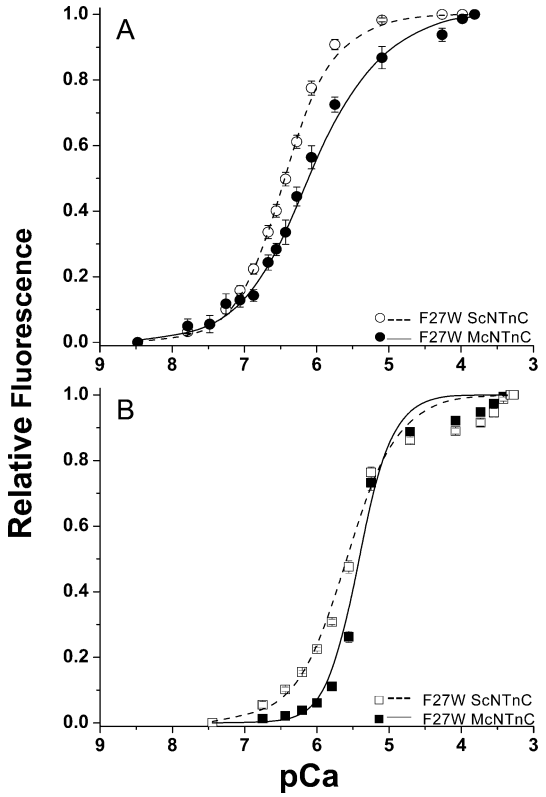

FIGURE 9: Comparison of the Ca^{2+} titration curves of F27W ScNTnC and F27W McNTnC at 30 °C, pH 7.0 and 7 °C, pH 7.0; determined using fluorescence to monitor Ca^{2+} binding. Data are normalized with respect to the maximal fluorescence of each Ca^{2+} titration and presented as mean ± SE. The curves generated by fitting the data with the Hill equation have been added to the figures for comparison against the data points. (A) Titration of fluorescence of F27W ScNTnC ($n = 9$), F27W McNTnC ($n = 6$) at 30 °C pH 7.0. (B) Titration of fluorescence of F27W ScNTnC ($n = 8$), F27W McNTnC ($n = 8$) at 7 °C pH 7.0.

capable of coordinating Ca^{2+} in other positions within an EF-hand. Position *y* still has a hydrophobic residue, but negative residues before (Asp 30) and after (Glu 32) may provide alternative binding, in an unusual EF-hand conformation. Titration of a number of F27W ScNTnC mutants while monitoring fluorescence has demonstrated that both Gln 29 and Asp 30 are required for F27W ScNTnC to maintain its high affinity for Ca^{2+} (*6*). This result suggests that both of these residues are involved in conferring ScNTnC its unique Ca^{2+} binding abilities.

The ability of site I of the sNTnC mutant E41A to bind Ca^{2+} has been previously characterized to examine the role site I plays in the Ca^{2+} activated conformational change of sTnC. This study by Li et al. (*9*) demonstrated that while the E41A mutation decreased the Ca^{2+} affinity of site I by 100 times, it did not completely eliminate the binding. The replacement of glutamate at residue 41 with alanine removes the coordinating residue in the $-z$ position through which bidentate coordination with the Ca^{2+} ion occurs through both carboxylate oxygens. These authors suggested that site I could still bind Ca^{2+} in the E41A mutant as the remaining five ligands at positions *x*, *y*, *z*, $-y$, and $-x$ were able to coordinate the Ca^{2+} ion. The calcium titration curve of G34 of ScNTnC is similar in shape to the corresponding residue in E41A sNTnC, G35 (*9*). Although the rate of change of the descending limb of the curve is much steeper for the E41A sNTnC mutant indicating a higher affinity of site I for Ca^{2+}, this still supports the suggestion that site I is capable of binding Ca^{2+} in ScNTnC.

The F27W mutation of ScNTnC appears to have an effect on the structure and function of site I, as indicated by the difference in chemical shift of the two proteins when they were in the same state (apo or one-Ca^{2+}-bound) and the difference in absolute chemical shift change during the Ca^{2+} titration. The difference in the chemical shift of I26 between [^{15}N] ScNTnC and [^{15}N]F27W ScNTnC is maintained whether the proteins were Ca^{2+} saturated or not, suggesting that this residue is affected by the mutation in both apo and Ca^{2+}-bound states. Other residues in site I, including Q29, A31, and E32, had different chemical shift values in the apo state, between wild type [^{15}N] ScNTnC and [^{15}N]F27W ScNTnC. These differences then disappeared once site II became saturated indicating that the two proteins have a similar structure in the Ca^{2+}-bound state. This suggests that the conformation of site I in apo [^{15}N]F27W ScNTnC is closer to the one Ca^{2+}-bound state than in wild type [^{15}N] ScNTnC. The larger chemical shift changes of the residues composing site I during Ca^{2+} binding to site II, including F27, Q29, A31, and E32, in wild type [^{15}N] ScNTnC indicate that the structural transition of site I is larger in [^{15}N] ScNTnC than in [^{15}N]F27W ScNTnC during Ca^{2+} activation. As a smaller conformational change needs to occur in this area of the protein in [^{15}N]F27W ScNTnC, a smaller energy barrier (ΔG) needs to be overcome. This probably results in a higher affinity for Ca^{2+} in [^{15}N]F27W ScNTnC. This result, however, does not invalidate the results of fluorescence studies (including the present, in which F27W cTnC mutants are used to quantify differences in Ca^{2+} affinity of different isoforms), as any effect of this mutation should be similar between isoforms.

The decrease in the Ca^{2+} affinity of F27W ScNTnC and F27W McNTnC when titration temperature was decreased from 30 to 7 °C is consistent with what has been reported for the full-length isoforms, as is the difference in Ca^{2+} affinities between the two proteins at both temperatures (*3*). This result demonstrates that temperature affects the Ca^{2+} affinity of the N-terminal domain in the same way whether the C-terminal domain is present or not and that the difference in Ca^{2+} affinity between the 2 isoforms is maintained without the C-terminal domain.

In summary, the results of the current study demonstrate that (i) site I is capable of binding Ca^{2+} in ScNTnC at high [Ca^{2+}], (ii) Ca^{2+} affinity for site II in ScNTnC decreases when assay temperature is decreased from 30 to 7 °C, as seen for the whole trout cardiac TnC (*3*), and (iii) the F27W mutation affects the apo structure and probably the Ca^{2+} affinity of ScNTnC.

Site I affinity was not detected using fluorescence techniques since the low affinity puts the binding out of the assay range. The dissociation constant can, however, be estimated from the binding curves obtained with NMR data (Figure 3), to be in the range of pCa of 2 to 3. This affinity is too low to make site I an effective Ca^{2+}-binding site in physiological conditions, but might be increased in the presence of TnI. Alternatively, the differences between trout and mammalian cardiac TnC can have a different effect that would improve the muscle sensitivity at lower temperatures, for instance, increasing the affinity for TnI.

ACKNOWLEDGMENT

We thank Gerry McQuaid for keeping the NMR spectrometers at top performance. The authors would also like to thank Dr. J. S. Ballantyne for the use his spectrofluorometer.

REFERENCES

1. Churcott, C. S., Moyes, C. D., Bressler, B. H., Baldwin, K. M., and Tibbits, G. F. (1994) *Am. J. Physiol. 267*, R62−70.
2. Moyes, C. D., Borgford, T., LeBlanc, L., and Tibbits, G. F. (1996) *Biochemistry 35*, 11756−11762.
3. Gillis, T. E., Marshall, C. R., Xue, X. H., Borgford, T. J., and Tibbits, G. F. (2000) *Am. J. Physiol. 279*, R1707−1715.
4. Krudy, G. A., Brito, R. M., Putkey, J. A., and Rosevear, P. R. (1992) *Biochemistry 31*, 1595−1602.
5. van Eerd, J. P., Capony, J. P., Ferraz, C., and Pechere, J. F. (1978) *Eur. J. Biochem. 91*, 231−242.
6. Gillis, T. E., Moyes, C. D., and Tibbits, G. F. (2003) *Am. J. Physiol: Cell Physiol. 283*, C1176−C1184.
7. Harrison, S. M., and Bers, D. M. (1990) *Am. J. Physiol. 258*, C282−288.
8. Tsuda, S., Miura, A., Gagne, S. M., Spyracopoulos, L., and Sykes, B. D. (1999) *Biochemistry 38*, 5693−5700.
9. Li, M. X., Gagne, S. M., Spyracopoulos, L., Kloks, C. P., Audette, G., Chandra, M., Solaro, R. J., Smillie, L. B., and Sykes, B. D. (1997) *Biochemistry 36*, 12519−12525.
10. Gagné, S. M., Tsuda, S., Li, M. X., Chandra, M., Smillie, L. B., and Sykes, B. D. (1994) *Protein Sci. 3*, 1961−1974.
11. Li, M. X., Gagne, S. M., Tsuda, S., Kay, C. M., Smillie, L. B., and Sykes, B. D. (1995) *Biochemistry 34*, 8330−8340.
12. Delaglio, F., Grzesiek, S., Vuister, G. W., Zhu, G., Pfeifer, J., and Bax, A. (1995) *J. Biomol. NMR 6*, 277−293.
13. Johnson, B., and Blevins, R. (1994) *J. Biomol. NMR 4*, 603−614.
14. Baudet, S., Hove-Madsen, L., and Bers, D. M. (1994) *Methods Cell. Biol. 40*, 93−113.
15. Bers, D. M., Patton, C. W., and Nuccitelli, R. (1994) in *A Practical Guide to the Study of Calcium in Living Cells* (Nuccitella, R., Ed.) pp 3−29, Academic Press, New York.
16. Campbell, A. P., and Sykes, B. D. (1991) *J. Mol. Biol. 222*, 405−421.
17. Spyracopoulos, L., Li, M. X., Sia, S. K., Gagne, S. M., Chandra, M., Solaro, R. J., and Sykes, B. D. (1997) *Biochemistry 36*, 12138−12146.
18. Baxter, N. J., and Williamson, M. P. (1997) *J. Biomol. NMR 9*, 359−369.
19. Cierpicki, T., and Otlewski, J. (2001) *J. Biomol. NMR 21*, 249−261.
20. Sia, S. K., Li, M. X., Spyracopoulos, L., Gagne, S. M., Liu, W., Putkey, J. A., and Sykes, B. D. (1997) *J. Biol. Chem. 272*, 18216−18221.
21. Blumenschein, T. M. A., Gillis, T. E., Tibbits, G. F., and Sykes, B. D. (2002) *Biophys. J. 82*, 387(a).
22. Gagne, S. M., Tsuda, S., Li, M. X., Smillie, L. B., and Sykes, B. D. (1995) *Nat. Struct. Biol. 2*, 784−789.
23. da Silva, A. C., and Reinach, F. C. (1991) *Trends. Biochem. Sci. 16*, 53−57.

BI0340494